Solute−Solvent Complex Switching Dynamics of Chloroform between Acetone and Dimethylsulfoxide−Two-Dimensional IR Chemical Exchange Spectroscopy

Kyungwon Kwak, Daniel E. Rosenfeld, Jean K. Chung, and Michael D. Fayer*

Department of Chemistry, Stanford University, Stanford, California 94305

Received: July 8, 2008; Revised Manuscript Received: August 28, 2008

Hydrogen bonds formed between C−H and various hydrogen bond acceptors play important roles in the structure of proteins and organic crystals, and the mechanisms of C−H bond cleavage reactions. Chloroform, a C−H hydrogen bond donor, can form weak hydrogen-bonded complexes with acetone and with dimethylsulfoxide (DMSO). When chloroform is dissolved in a mixed solvent consisting of acetone and DMSO, both types of hydrogen-bonded complexes exist. The two complexes, chloroform−acetone and chloroform−DMSO, are in equilibrium, and they rapidly interconvert by chloroform exchanging hydrogen bond acceptors. This fast hydrogen bond acceptor substitution reaction is probed using ultrafast two-dimensional infrared (2D-IR) vibrational echo chemical exchange spectroscopy. Deuterated chloroform is used in the experiments, and the 2D-IR spectrum of the C−D stretching mode is measured. The chemical exchange of the chloroform hydrogen bonding partners is tracked by observing the time-dependent growth of off-diagonal peaks in the 2D-IR spectra. The measured substitution rate is 1/30 ps for an acetone molecule to replace a DMSO molecule in a chloroform−DMSO complex and 1/45 ps for a DMSO molecule to replace an acetone molecule in a chloroform−acetone complex. Free chloroform exists in the mixed solvent, and it acts as a reactive intermediate in the substitution reaction, analogous to a S_N1 type reaction. From the measured rates and the equilibrium concentrations of acetone and DMSO, the dissociation rates for the chloroform−DMSO and chloroform−acetone complexes are found to be 1/24 ps and 1/5.5 ps, respectively. The difference between the measured rate for the complete substitution reaction and the rate for complex dissociation corresponds to the diffusion limited rate. The estimated diffusion limited rate agrees well with the result from a Smoluchowski treatment of diffusive reactions.

I. Introduction

C−H groups can form hydrogen bonds with bases that act as hydrogen bond acceptors.[1] These weak yet directional interactions can stabilize important structures in biology and chemistry.[2,3] In simple organic solutions, C−H groups can also form short-lived hydrogen-bonded complexes with electron rich molecules. These complexes are especially strong when the C−H group is activated by neighboring electron withdrawing groups. Such activated C−H groups are acidic enough to form complexes with weak hydrogen bond acceptors such as the delocalized π-electrons in benzene. In this study we examine hydrogen-bonded complexes composed of deuterated chloroform ($CDCl_3$) and either acetone or dimethylsulfoxide (DMSO). When the deuterated chloroform solute is dissolved in a mixed solvent of acetone and DMSO, the two distinct complexes are in equilibrium. Chloroform switches back and forth between acetone and DMSO partners.

The properties of C−H hydrogen bonding have been studied previously using thermodynamic measurements, X-ray scattering,[4,5] neutron scattering,[2,6] and IR,[1,7] and NMR[1,8] spectroscopy. Neutron scattering permits the accurate determination of hydrogen positions in organic and protein crystals. The observation of short distances between C−H hydrogens and electronegative atoms has provided evidence for C−H hydrogen bonding in crystals.[2] NMR studies have also revealed a change in C−H chemical shift upon the addition of hydrogen bond acceptors. This change is attributed to hydrogen bonding, where the new chemical shift is the strongly motionally narrowed average of the chemical shifts of the hydrogen-bonded and non-hydrogen-bonded states.[9−11] Infrared absorption spectroscopy is a useful method for studying hydrogen bonding because the frequency and extinction coefficient of the hydrogen bond donating group's stretching band is sensitive to the presence and strength of the hydrogen bond.[12] IR spectroscopy can be used to observe a molecule in both hydrogen-bonded and non-hydrogen-bonded states because usually the states have different vibrational frequencies. Furthermore, since the time scale of the spectroscopic probe is on the order of the optical period, IR spectra of such systems show clearly resolved peaks, whereas in NMR the peaks are strongly motionally narrowed and only one peak is observed. For most hydrogen bonding systems, vibrational frequencies are red-shifted upon complex formation. Because C−H groups are weakly acidic, its hydrogen bonding strength, and thus the associated red-shift in C−H (or C−D) stretching frequency, is typically small, which can impede spectral assignment and interpretation. Despite small C−H stretch frequency shifts, IR spectroscopy has been one of the major tools used to study C−H hydrogen bonding as well as other hydrogen bonding systems.[13,14]

Recently a considerable amount of interest has arisen over C−H···O and C−H···π hydrogen bonds because these two types of hydrogen bonds appear frequently in biomolecules and are partly responsible for the macromolecular structures of proteins.[3] C_α−H···O hydrogen bonding is of particular importance in transmembrane helix association.[15] The strength of

* To whom correspondence should be addressed. E-mail: fayer@stanford.edu.

10.1021/jp806035w CCC: $40.75
Published on Web 10/15/2008

C_α−H···O hydrogen bonding in a lipid bilayer was studied recently using IR spectroscopy.[16] The C−H···O hydrogen bond strength is usually comparable to room temperature thermal energy, so the dissociation and formation of hydrogen bonds can occur readily. Therefore, fast fluctuations of a biomolecule's global structure can involve rapid continual formation and dissociation of C−H hydrogen bonds. In addition to its importance in biology, C−H hydrogen bonding has been proposed as the main factor in determining the high stereo selectivity of Diels−Alder reactions using Lewis acid catalysts.[17] Also, some reactions, including C−H activation, are expected to have a hydrogen bond to the C−H as an intermediate.[18]

Because the enthalpy of formation of C−H···O hydrogen bonds is small, room temperature association and dissociation dynamics are anticipated to occur on very fast timescales. Ultrafast two-dimensional infrared (2D-IR) vibrational echo chemical exchange spectroscopy (CES) has proven to be a valuable tool for studying fast chemical exchange processes under thermal equilibrium conditions.[19−26] Earlier studies of organic solute−solvent complex dynamics using 2D-IR CES examined complexes formed between alcohol solutes and aromatic solvents by observing the alcohols' hydroxyl stretching mode.[19−26] The complexes studied here have weaker bonds. Even though the interaction energies of C−H hydrogen bonds are only slightly greater than a Van der Waals interaction, their directionality plays a significant role in determining the structure of organic crystals and the secondary structure of membrane proteins. Here, the formation and dissociation of solute−solvent complexes and the details of the switching of the solute chloroform between its mixed solvent partners acetone and dimethylsulfoxide were observed by tracking the growth of the off-diagonal peaks in time−dependent 2D-IR spectra of the C−D stretch. A previous experimental study attempted to measure the C−H···O hydrogen bond dynamics between N-methylacetamide (NMA) and $CDCl_3$ with 2D-IR spectroscopy by observing the amide mode (N−C═O).[27] MD simulation of NMA/$CDCl_3$ suggested that the broad amide I band of NMA dissolved in $CDCl_3$ is composed of three species, NMA···$CDCl_3$, NMA···$(CDCl_3)_2$, and NMA···$(CDCl_3)_3$. However, because the amide I band was so broad and almost featureless, no clear evidence of off-diagonal peaks or the growth of off-diagonal peaks was observed experimentally.[27]

We observe C−H hydrogen bond partner substitution dynamics, chloroform switching between acetone and DMSO, in real time. The two complexes interconvert by chloroform breaking the hydrogen bond with one acceptor and making a hydrogen bond with the other acceptor. The growth of off-diagonal peaks in the 2D-IR vibrational echo spectra is the direct result of this general substitution reaction. The observed rates for the entire substitution reaction are converted to concentration independent second-order rate constants, which are related to the elementary process of hydrogen bond breaking. The difference between the measured rate and the rate for hydrogen bond breaking is the time for $CDCl_3$ to find a new hydrogen bonding partner. This search process is controlled by diffusion. Using the diffusion limited rate constants and dissociation times for each complex, we are able to reproduce the kinetics within experimental error. The results yield a kinetic scheme for the ultrafast substitution reaction.

II. Results and Discussion

A. Infrared Absorption Spectra. The linear IR spectrum of a hydrogen bond donor's stretching band is typically characteristic of its hydrogen bonding state. The red shift of the peak frequency and the increase in transition dipole render a distinct IR spectrum when compared with the IR spectrum without hydrogen bonding. Chloroform can act as a C−H hydrogen bond donor, but the peak position of the C−H stretching band overlaps with many other C−H related vibrational bands from the methyl groups of acetone and DMSO. Therefore, the hydrogen of chloroform was replaced with deuterium to obtain a clean spectral window for the IR and 2D-IR measurements. When the deuterated chloroform ($CDCl_3$) is dissolved in the mixed solvent composed of acetone and dimethylsulfoxide, the C−D stretching band associated with the chloroform−DMSO complex appears at a lower frequency than the band for the chloroform−acetone complex (see Figure 1A). The mole fraction of each molecule in the sample is given by the ratio 1:5:26 ($CDCl_3$−DMSO−acetone). In Figure 1A, the C−D stretching bands of $CDCl_3$ in pure DMSO and pure acetone are plotted together with the C−D stretching spectrum in the mixed solvent. The absorption band at high frequency matches the spectrum of $CDCl_3$ in pure acetone, so it is assigned to the chloroform−acetone complex. The low frequency band is not identical to the C−D absorption band in pure DMSO; it shows a blue shift in maximum frequency of about 4 cm^{-1}. The addition of the two chloroform bands measured in pure acetone and pure DMSO does not perfectly reproduce the spectrum in the mixed solvent. Also, the C−D stretching bands in pure DMSO and pure acetone have distinctly asymmetric line shapes, specifically, there are tails to the low frequency side of the bands. These tails suggest that there is an inhomo-

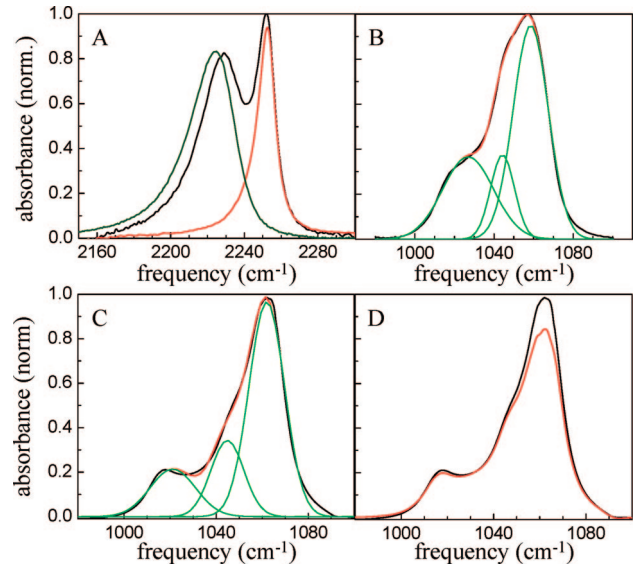

Figure 1. The linear IR spectra for determining the hydrogen bond structure of $CDCl_3$ in the mixed solvent acetone/DMSO. (A) Black: C−D stretching spectrum of 6 wt % $CDCl_3$ in the mixed solvent acetone/DMSO (weight ratio 80:20). The mole ratio is 1:26:5 ($CDCl_3$−acetone−DMSO). Green: C−D stretching band of 6 wt % $CDCl_3$ in pure DMSO. Red: C−D stretching spectrum of 6 wt % $CDCl_3$ in pure acetone. The absorbance scale is normalized to the largest peak. The maximum optical density of $CDCl_3$ in the mixed solvent is 0.35. (B) The S═O stretching spectrum of pure DMSO (black). The entire spectrum is well fit by three Gaussian functions (green). The three Gaussians are shown (red). (C) The S═O stretching spectrum (black) in the mixed solvent (acetone/DMSO) is also well fit by three Gaussian functions (green). The mixed solvent does not change the structure of S═O stretching band substantially, but the contribution from the linear dimer (low frequency peak) is smaller. (D) The S═O stretching absorption of the DMSO in 6 wt % $CDCl_3$ in the mixed solvent (red) is compared with the S═O stretching band of the mixed solvent without $CDCl_3$ (black).

geneous distribution of chloroform hydrogen bonding structures. To obtain a detailed assignment of the spectra and to understand the line shape of each absorption peak in the mixed solvent, the IR spectra of $CDCl_3$ in various different solvents were measured and analyzed.

1. Determination of the Complexes' Structures. The blue shift of the chloroform C−D stretching frequency in the mixed solvent relative to the frequency in pure DMSO is induced by the change in the DMSO cluster structure. The blue shift of the peak frequency in a hydrogen-bonded molecule is mainly attributed to weakening of the hydrogen bonding. However, it is not clear why the presence of acetone around a chloroform−DMSO complex reduces the hydrogen-bonding strength between the $CDCl_3$ and DMSO as observed in the mixed solvent. The higher frequency peak in Figure 1A shows little change compared with the $CDCl_3$ spectrum in pure acetone presumably because acetone occupies ∼85% of the mixed solvent volume, so there is little change from pure acetone. In contrast, the environment around the chloroform−DMSO complex in the mixed solvent is very different from that found in pure DMSO.

DMSO and acetone are highly associative molecules. They have large dipole moments and strong intermolecular interactions. The self-association of acetone and DMSO in the pure liquids has been extensively studied.[28−33] In both liquids, the molecules primarily exist as cyclic (dipoles antialigned) and linear (dipoles aligned) dimers stabilized by the dipole−dipole interaction.[28,32,33] The liquid structure of DMSO is particularly interesting because of the unusual properties of DMSO as a solvent.[33] Raman spectroscopy of the S═O stretching band of DMSO suggests that there are three different cluster structures plus a monomer.[32] The IR spectrum of the S═O stretching mode in pure DMSO (see Figure 1B) shows three distinct features related to the cyclic and linear dimers, in agreement with the previous Raman results.[32,34] The spectrum in Figure 1B can be decomposed into three Gaussian peaks centered at, 1058, 1044, and 1027 cm^{-1}. These peaks agree with the Raman spectrum which displays bands at 1057, 1042, and 1027 cm^{-1}.[32,34] The two high frequency peaks and the low frequency peak arise from the cyclic and linear dimer respectively. In the DMSO/acetone mixed solvent, the S═O spectrum (Figure 1C) is slightly different than that in pure DMSO but the three distinctive structures are largely preserved. The band is again well fit by three Gaussian functions (centers: 1062, 1046, and 1021 cm^{-1}). In the mixed solvent, the ratio of the areas of the high and low frequency peaks is larger than in the pure solvent. The ratio of the cyclic and linear dimers changes from 1.8 in pure DMSO to 4 in the mixed solvent. The ratio of the two cyclic dimer peaks (high and middle frequencies) is very similar in DMSO (3.7) and the mixed solvent (3.2). This change demonstrates that the population of the cyclic dimer is enhanced in the mixed solvent.

The S═O stretching spectra in the DMSO/acetone mixed solvent with and without $CDCl_3$ are compared in Figure 1D. Because the IR spectrum of the hydrogen bond acceptor is sensitive to the formation of the hydrogen bond, the S═O spectrum will change when $CDCl_3$ is added to the mixed solvent. The cyclic dimer S═O stretching changes significantly but there is little change in the linear dimer peak. This result shows that $CDCl_3$ hydrogen bonds primarily with the DMSO cyclic dimer. When the mixed solvent is highly diluted with CCl_4, the band for the monomer (1071 cm^{-1}) grows in intensity, as is expected from the prior Raman studies.

The spectroscopic results show that $CDCl_3$ mainly hydrogen bonds with the cyclic dimer although two different structures of DMSO exist in the mixed solvent. Acetone is also known to form a cyclic dimer mainly through the hydrogen bonding between the C═O on one acetone and a hydrogen from the methyl group on another acetone.[28,29] When $CDCl_3$ is dissolved in acetone, $CDCl_3$ forms a second hydrogen bond to a C═O of acetone which is already accepting a hydrogen bond from a methyl group hydrogen. Thus, in the mixed solvent, the C−D of $CDCl_3$ primarily hydrogen bonds to two species, the DMSO cyclic dimer and the acetone dimer. There may be a very minor population of $CDCl_3$ hydrogen bonded with a linear dimer, but it can be ignored because of its very low concentration. The equilibrium structures of hydrogen bond complexes were calculated without solvent using DFT at the B3LYP/6-311++G(d,p) level of theory. The structures are shown in Figure 2.

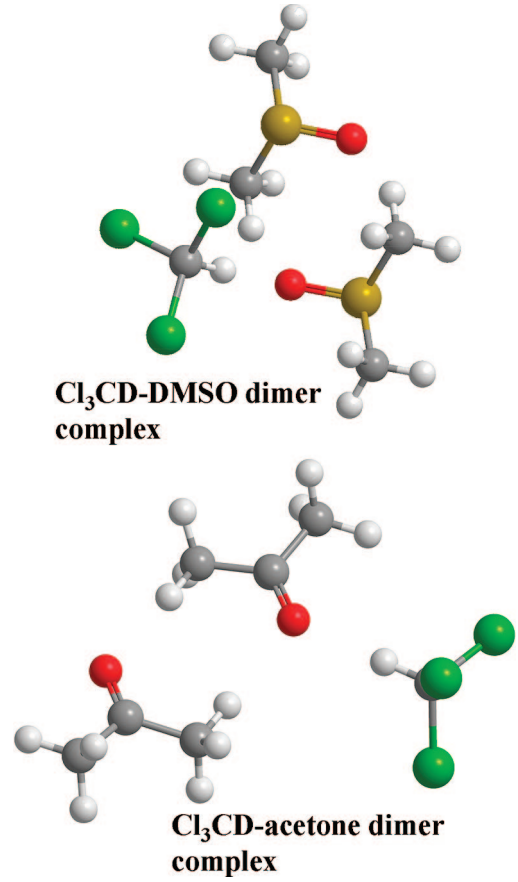

Figure 2. Structures of the complexes determined from electronic structure calculations (DFT with 6-311++G(d,p) basis set) with no solvent. Both complexes have $CDCl_3$ hydrogen bonded to one of the oxygens of a dimer. DMSO forms a cyclic dimer because of dipole−dipole interactions. [32,33] Acetone also forms a cyclic dimer because of a hydrogen bond C_α−H···O, where the C−H is on one acetone and the O is on the other. $CDCl_3$ makes a second hydrogen bond with one of the oxygen atoms of the dimer.

2. Determination of Equilibrium Using the C−D Bending Spectrum. The measurements discussed above demonstrate that the two C−D stretching peaks observed in the DMSO/acetone mixed solvent (Figure 1A) come from the chloroform−DMSO complex and the chloroform−acetone complex. Because acetone and DMSO form weak hydrogen bonds with $CDCl_3$, we cannot rule out the existence of free $CDCl_3$ (not complexed) in the mixed solvent. The IR absorbance from free $CDCl_3$ should be observable or affect the measured spectrum if there is a significant amount of free $CDCl_3$. The peak position of free $CDCl_3$ was determined from the spectrum of $CDCl_3$ in pure

CCl_4 to avoid self-association of $CDCl_3$ through very weak hydrogen bonding between C−D and C−Cl.[35] The free $CDCl_3$ (2253 cm^{-1}) has almost the same peak position as that of the $CDCl_3$−acetone complex, but the C−D stretch absorption coefficient of the free form is much smaller than that of the complex.

Both the thermodynamics and spectroscopy of the association of chloroform with acetone have been previously studied.[1,2] The hydrogen bonding of chloroform and acetone is evidenced by the deviation of solution behavior from the ideal.[12] However, quantitative NMR and IR measurements of the equilibrium constant between free acetone and the chloroform−acetone complex produce a wide range of values.[36,37] Both IR and NMR techniques experience difficulty with the chloroform−acetone system. First, the use of NMR to determine the equilibrium concentrations of two species is hampered by motional narrowing, which merges the peaks of the two species. Second, though the hydrogen bonding formation enhances the IR extinction coefficient of the C−D stretching band, there is little frequency separation between the free $CDCl_3$ and complexed $CDCl_3$.[14] The negligible frequency separation results in a single peak that is completely dominated by the complex. In the mixed solvent, the stronger chloroform−DMSO hydrogen bond will further reduce the concentration of free chloroform compared to a pure acetone solvent, and the chloroform−DMSO spectrum overlaps the chloroform−acetone spectrum. To overcome these difficulties, we first determined the concentration of free chloroform in pure acetone using the C−D bending mode rather than the stretching mode. The equilibrium constant for the reaction

$$CDCl_3 + (CH_3)_2C{=}O \overset{K}{\rightleftharpoons} Cl_3CD\cdots O{=}C(CH_3)_2$$

is obtained. The equilibrium concentration of free chloroform in acetone gives us the upper limit of the free chloroform concentration in the mixed solvent because the addition of a stronger hydrogen bonding acceptor, DMSO, will shift the equilibrium toward less free chloroform.

Using the C−D bending mode of chloroform to measure the equilibrium concentrations is advantageous for two reasons. First, the difference in the peak frequencies of the free and complexed C−D bending mode is greater than it is for the stretching mode. Second, the difference in the absorption coefficients of the free and complexed C−D bend is small, so the presence of the free species in the IR spectrum is apparent. Figure 3A shows the C−D bending spectrum of $CDCl_3$ in CCl_4 (red), acetone (black), and DMSO (green). The C−D bending mode peak blue shifts upon hydrogen bond formation, and the absorption coefficient decreases. The integrated absorption coefficient of the C−D bending mode in CCl_4 is obtained from the measured spectrum, $\varepsilon_{C-D}(CCl_4) = 5030\ cm^{-1}\cdot L/mol$. If we assume that only a very small amount of the $CDCl_3$ exists as the free form in acetone or DMSO, the integrated absorption-coefficient is $\epsilon_{C-D}(acetone) = 4081\ cm^{-1}\cdot L/mol$ and $\epsilon_{C-D}(DMSO) = 2334\ cm^{-1}\cdot L/mol$. Because the molar absorptivity of the bending motion decreases upon the formation of a hydrogen bond, the free species' signature should appear clearly in the IR bend spectrum of $CDCl_3$. For $CDCl_3$ in pure acetone, the C−D bending band has a tail with a small shoulder on the low frequency side (Figure 3B, dark blue curve). Because the position of this tail matches the frequency of free $CDCl_3$ in pure CCl_4, it can be assigned to the free $CDCl_3$ that exists in pure acetone. This assignment can be confirmed by taking the spectrum in an acetone/CCl_4 mixed solvent (Figure 3B, green curve). The C−D bending spectrum shows a clear peak for free $CDCl_3$ following the addition of CCl_4 at the same position as the C−D bend in CCl_4. The C−D bending spectrum was also measured in 2-,2-,4-,4-tetramethyl, 3-pentanone, an analogue of acetone, which forms a weaker hydrogen bond with $CDCl_3$. The cyan curve in Figure 3B clearly shows the presence of additional free $CDCl_3$ when this more weakly interacting solvent is used. For comparison, the bending spectrum of $CDCl_3$ in the mixed solvent is also plotted in Figure 3B (black curve).

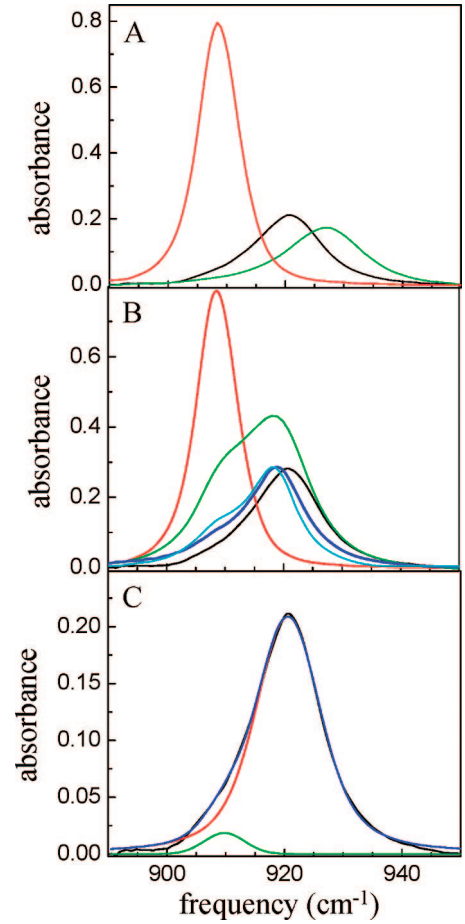

Figure 3. The C−D bending spectrum for determining the equilibrium constant between free $CDCl_3$ and the $CDCl_3$−acetone complex dissolved in acetone. (A) The C−D bending spectrum of 5 wt % $CDCl_3$ in acetone (black), DMSO (green), and CCl_4 (red). The C−D bending spectrum shows the opposite trend than the C−D stretching spectrum. Formation of a hydrogen bond blue shifts the frequency, and the absorption coefficient decreases. (B) The C−D bending spectra in various solvents show that the C−D bending frequency changes depending upon solvent. Five wt % $CDCl_3$ in the mixed solvent (black), acetone (blue), 2-,2-,4-,4-tetramethyl, 3-petanone (cyan), in the CCl_4/acetone (mole ratio 45/55, green), and CCl_4 (red). (C) The C−D bending spectrum of 5 wt % $CDCl_3$ in acetone is decomposed into two peaks. The center frequency of the small Gaussian peak is almost identical to the peak position of free $CDCl_3$ measured in the pure CCl_4 (909 cm^{-1}).

The IR spectrum of the C−D bending mode was measured with both 5 and 10 wt % $CDCl_3$ in pure acetone. First, the spectrum from the 5 wt % of $CDCl_3$ in acetone sample (Figure 3C, black curve) was analyzed. The blue side of the spectrum was fit using a Voight function. The resulting Voight function is shown over the full spectral range (red curve). The difference between the IR spectrum and the fit spectrum is assigned to the free $CDCl_3$ in pure acetone (green curve). This curve is Gaussian

in form. The addition of this Gaussian function and the Voight function reproduces the observed IR spectrum well (blue curve). Using Beer's law, the concentration of free $CDCl_3$ can be calculated using the molar absorption coefficient for $CDCl_3$ in pure CCl_4. The free $CDCl_3$ in acetone has a different dielectric environment than the free $CDCl_3$ in CCl_4, so the molar absorption coefficient must be corrected. The absorption coefficient in the solvent (ε_l) with refractive index, n_0, can be related to the absorption coefficient in gas phase (ε_g) taking the solute be spherical.[38]

$$\varepsilon_l = \frac{1}{n_0}\left[\frac{n^2+2}{(n/n_0)^2+2}\right]^2 \varepsilon_g \qquad (1)$$

Here n is the refractive index of the solute molecule. Using this equation, the molar absorption coefficient measured in the CCl_4 can be converted into the molar absorption coefficient for the acetone solution. The corrected molar absorption coefficient is ε_{C-D} (free chloroform in acetone) = 5289 cm^{-1}·L/mol. Using this value and the measured area, the concentration of free $CDCl_3$ in acetone is determined to be 0.013 mol/L, which corresponds to 3.7 mol % of the total $CDCl_3$. The spectrum from 10 wt % of $CDCl_3$ in acetone was measured and analyzed using the same methodology. The concentration of free $CDCl_3$ was calculated to be 3.6 mol %. Thus we conclude that 3.7 mol % of the $CDCl_3$ exists as the free species in pure acetone. This value is used as an upper limit of the free $CDCl_3$ in the DMSO/acetone mixed solvent. Because DMSO forms a stronger hydrogen bond with chloroform than acetone does, we expect the concentration of the free species to be less than the 3.7% determined in pure acetone. Our inability to detect the free $CDCl_3$ band in the bend spectrum in the mixed solvent suggests that the concentration of the free species is below 2%. The small but observable amount of free $CDCl_3$ measured in pure acetone supports the proposition discussed below that the free $CDCl_3$ acts as an intermediate in the kinetic pathway for the hydrogen bond acceptor substitution reaction.

B. Hydrogen Bonding Dynamics Studied by the 2D-IR. It has been shown previously that the formation and dissociation dynamics of hydrogen bonding complexes can be studied by measuring the growth of off-diagonal peaks in 2D-IR vibrational echo chemical exchange spectra.[20,21,24,39] The kinetic and thermodynamic details of the hydroxyl-π hydrogen-bonding complexes of phenols and benzene derivatives were studied in detail using 2D-IR CES combined with ab initio calculations, temperature dependent IR spectroscopy, and molecular dynamics simulations.[20,24,40] One important result is that an Arrhenius type rate law exists that relates the dissociation time of hydrogen-bonded complex to the enthalpy of formation of the complex. The experiments were extended to triethylsilanol complexes with benzene derivatives.[39] The same relationship was found between the dissociation time and the enthalpy of formation. In all, thirteen phenol and silanol complexes fell on the same line relating the dissociation time to the enthalpy of formation.[39]

In the previous studies of solute−solvent dynamics, mixed solvents were used, but the solute could only form a hydrogen bond with one of the components of the mixed solvent. Here the solute, $CDCl_3$, can form a hydrogen bond with both the DMSO and acetone components of the mixed solvent. The solute switches from being bound to one type of molecule to the other. Therefore, the over all process is akin to a chemical substitution reaction. A general hydrogen bond substitution reaction occurs in three distinct elementary steps: breaking the hydrogen bond with the old partner, species diffusion to find a new partner, and formation of the hydrogen bond with the new partner. The chloroform in the DMSO/acetone C−D···O hydrogen bond system displays these three elementary steps, which can be explicated using 2D-IR CES.

The 2D-IR vibrational echo chemical exchange method including the experimental setup and data processing has been previously described in detail.[20,21,25,41] For completeness, the method will be described briefly. In a 2D-IR vibrational echo experiment, three ultrafast mid-IR pulses with ~60 fs duration, tuned to the frequency range of the vibrational modes of interest, are crossed in the sample. The broad bandwidth (fwhm 250 cm^{-1}) makes it possible to simultaneously excite a number of vibrational bands. The first laser pulse places the vibrational oscillators into a coherent superposition of the ground and the first excited states. This coherence period labels the initial structure of the species in the sample by setting their initial frequencies along the $\omega_\tau$axis of the 2D spectrum. The second pulse ends the first time period τ by transforming the coherences into populations (either in the ground state or first excited state) and starts clocking the reaction time period T_w during which the labeled species undergo chemical exchange, that is, hydrogen bond partner substitution. Chemical exchange also occurs during the coherence periods, but such exchange does not contribute to off-diagonal peaks and since these periods are short compared to T_w exchange during these times is assumed to be negligible. The chemical exchange is manifested in the 2D spectrum by changes in the vibrational frequencies of the vibrational modes under study; these changes are manifested as off-diagonal peaks in the 2D spectra. The third pulse ends the population period of length T_w and begins a third period of length $\leq \tau$, which ends with the emission of the vibrational echo pulse with the frequencies along the ω_m axis of the 2D spectrum. The vibrational echo pulse is the signal in the experiment. The vibrational echo is measured for both rephasing and nonrephasing pathways ($\tau > 0$ and $\tau < 0$, respectively), and the real part is taken of the sum of both pathways. This results in nearly purely absorptive spectra.

The vibrational echo pulse reads out information about the final structure of all labeled species by their ω_m frequencies. During the period T_w between pulses 2 and 3, chemical exchange occurs. The exchange causes new off-diagonal peaks to grow in as T_w is increased. The growth of off-diagonal peaks in the 2D spectra with increasing T_w is used to extract the exchange reaction times. In addition to chemical exchange, other population dynamics such as vibrational relaxation to the ground-state and orientational relaxation of the entire molecule will influence the 2D spectrum. Vibrational relaxation and orientational relaxation cause all peaks to decrease in amplitude. Chemical exchange causes the off-diagonal peaks to grow in amplitude. The vibrational relaxation and orientational relaxation are measured separately using IR pump−probe experiments. All of these dynamics processes are included in the data analysis.

Several examples of the 2D-IR spectra are plotted in Figure 4. Only the portions of the spectra arising from the ground vibrational states to the first excited vibrational states (0-1) are shown. Previously it has been shown that the 0-1 and 1-2 portions of the spectra provide the same information and that vibrational excitation does not change the thermal equilibrium dynamics of the chemical exchange system.[20] In cases where the anharmonicity of the vibrations is small relative to the fwhm of the 2D peaks, all eight peaks arising from the 0-1 and 1-2 transition must be included in the analysis due to destructive interference. In this case, the anharmonicity of the C−D

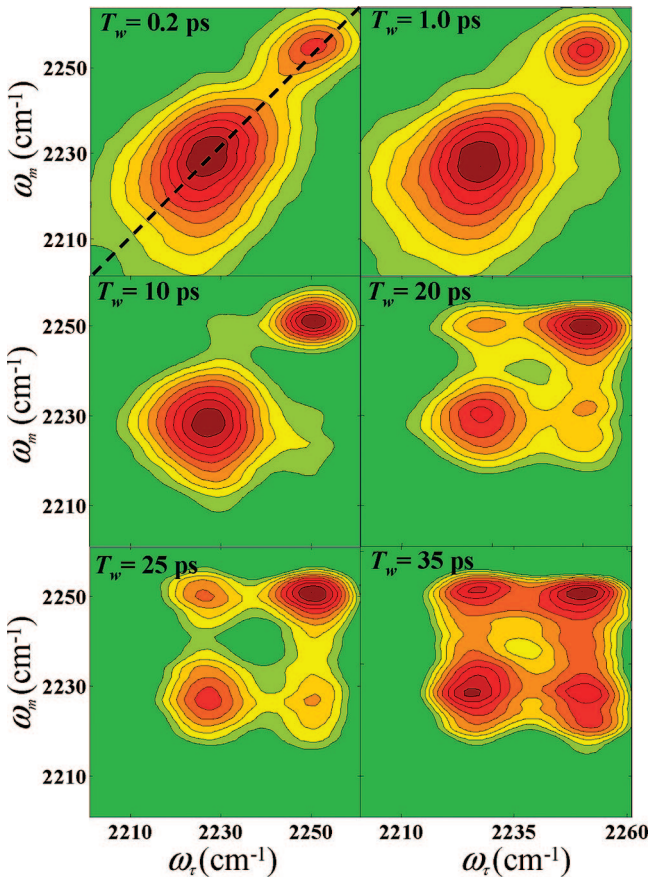

Figure 4. Absorptive 2D-IR vibrational echo spectra of the C−D stretching mode of $CDCl_3$ in the mixed solvent, acetone/DMSO. The spectra are the real part of the sum of the rephrasing and nonrephasing pathways. Only the peaks from the 0→1 transition are shown. The dashed line in the upper left-hand panel is the diagonal. As T_w increases, off-diagonal peaks grow in. The growth of the off-diagonal peaks provides a direct measure of the chemical exchange (partner substitution) between the $CDCl_3$−DMSO and $CDCl_3$−acetone complexes.

stretching mode is ∼70 cm^{-1}, which is greater than the fwhm of the 2D peaks. Therefore we only need to include the 0-1 peaks in the analysis. For T_w less than 2 ps, there are only two diagonal peaks. The diagonal is shown in the upper left-hand panel of Figure 4. Diagonal peaks reflect the populations of the species that have not undergone chemical exchange. The low frequency (on the ω_m axis) diagonal peak is proportional to the population of the chloroform−DMSO complex that has the same hydrogen bonding partner at the beginning and end of T_w, the population period. The high frequency diagonal peak arises from the population of chloroform−acetone complex that has the same hydrogen bonding partner at the beginning and end of T_w, the population period. The diagonal peak positions along the ω_m axis are the same as in the absorption spectrum (see Figure 1A). At short times, the diagonal peaks are elongated along the diagonal, which is an indication of inhomogeneous broadening. As T_w increases, thermally induced fluctuations in the structure of the complex and interactions with the surrounding solvent cause the frequency to evolve, that is, spectral diffusion to occur. Spectral diffusion changes the shapes of the peaks, but not their volumes.[21] In the data analysis, the time dependent volumes of the peaks are used in the chemical exchange analysis, eliminating the influence of spectral diffusion.[20,21] In the experiments presented here, spectral diffusion is fast compared to chemical exchange.

In Figure 4, off-diagonal peaks have begun to appear by 10 ps, and by 20 ps they are clearly evident. The off-diagonal peak at (ω_τ,ω_m) = (2229, 2252 cm^{-1}) comes from chloroform−DMSO complexes that became chloroform−acetone complexes. The off-diagonal peak at (2252, 2229 cm^{-1}) comes from chloroform−acetone complexes that became chloroform−DMSO complexes. The off-diagonal peak at (2252, 2229 cm^{-1}) (chloroform−acetone → chloroform−DMSO) is the result of three elementary processes: breaking the hydrogen bond between $CDCl_3$ and acetone to form a free $CDCl_3$, diffusion to an encounter between $CDCl_3$ and DMSO, and finally formation of the hydrogen-bonded chloroform−DMSO complex. The other off-diagonal peak follows the same sequence, chloroform−DMSO breaks, diffusion occurs, and chloroform−acetone forms. It is important to point out that if a complex breaks and reforms as the same type of complex, it does not contribute to an off-diagonal peak. Only net chemical exchange, in which one species turns into another, contributes to the growth of the off-diagonal peaks.

It is conceivable that the chemical exchange occurs without the free chloroform intermediate. A DMSO could collide with a chloroform−acetone complex with the proper orientation to form a three-center hydrogen-bonded transition state which has one donor, $CDCl_3$, and two acceptors, acetone and DMSO, or vice versa.[22] The distinction between these two kinetic schemes is the same as the difference between S_N1 and S_N2 reactions. Using the well-known substitution reaction mechanism as an analogy, the existence of the intermediate (free $CDCl_3$) that has already lost its leaving group is evidence supporting an S_N1 type reaction scheme. The presence of an appreciable amount of free $CDCl_3$ in pure acetone and the implication that free $CDCl_3$ also exists in the mixed solvent, which is 85% acetone by volume, indicates that the S_N1 reaction mechanism is probably appropriate. The detailed data analysis presented below will strongly support that the exchange reaction proceeds via a unimolecular process (S_N1) with free $CDCl_3$ as an intermediate.

To perform a detailed analysis of the 2D data, we need to know the equilibrium species present in the sample and their effect on the IR and 2D-IR spectra. As shown using the IR absorption measurements, there is expected to be less than ∼4% free $CDCl_3$ in the mixed solvent. The 2D-IR spectrum depends on the fourth power of the transition dipole or approximately the square of the absorption coefficient. The absorption coefficient of the C−D stretching mode of free $CDCl_3$ is so small that it does not contribute to the 2D-IR spectrum. The absorption coefficient of the stretching band of the free $CDCl_3$ is ε_{C-D} = 58.6 cm^{-1}·L/mol. This value is measured in pure CCl_4 to avoid possible self-association effects in pure $CDCl_3$. Because ∼4 mol% free $CDCl_3$ exists in pure acetone, only 96% of the initial $CDCl_3$ complexes with acetone. In pure acetone, the $CDCl_3$−acetone complex is the only contributor to the measured area of the IR spectrum because of the large difference in population and absorbance. The absorption coefficient was determined to be 1390 cm^{-1}·L/mol for the $CDCl_3$−acetone complex. The absorption coefficient of the C−D stretching band in pure DMSO was measured to be 3320 cm^{-1}·L/mol. This absorption coefficient was corrected for the change in dielectric medium in going from pure DMSO to the mixed solvent, which is mainly composed of acetone. The refractive index of the mixed solvent is calculated using the Lorentz-Lorenz, or Clausius-Mossotti equation, and then Equation 1 was used to correct for the change in dielectric environment.[42] The resulting C−D stretching absorption coefficient for the complex with DMSO in the mixed solvent is 3400 cm^{-1}·L/mol which is 2.5 times larger than that that of acetone. The population ratio of the two complexes was determined to be [chloroform−acetone]/

[chloroform−DMSO] = 0.66 using the absorption coefficients and the measured area for each complex peak in the C−D stretching spectrum (Figure 1A).

The time dependent behavior of all four peaks can be described using a kinetic model which includes exchange, vibrational relaxation, and orientational diffusion. Even though the exchange reaction is kinetically more complicated than the complex dissociation and formation reactions that have been studied previously,[20,21,24,39] the same kinetic equations for 2D-IR peaks can be applied to describe the time dependence of the diagonal and off-diagonal peaks. The net exchange reaction can be written as

$$Cl_3CD\cdots O{=}S(CH_3)_2 + (CH_3)_2C{=}O \underset{\xi'}{\overset{\xi}{\rightleftharpoons}} Cl_3CD\cdots O{=}C(CH_3)_2 + (CH_3)_2S{=}O \quad (2)$$

From the 2D-IR CES measurements, only the population changes of chloroform−DMSO and chloroform−acetone can be measured and related to concentration changes. Thus the net reaction we observe from the 2D-IR spectra is

$$Cl_3CD\cdots O{=}S(CH_3)_2 \underset{k'}{\overset{k}{\rightleftharpoons}} Cl_3CD\cdots O{=}C(CH_3)_2 \quad (3)$$

The rate constant k and k' can be expressed as $k = \xi \times$ [acetone] and $k' = \xi' \times$ [DMSO]. Note, k and k' depend on the equilibrium concentrations of acetone and DMSO, and these values depend on the concentrations used in sample preparation. At equilibrium, the concentrations of acetone and DMSO are constant, so k and k' can be treated as pseudo first-order reaction rate constants. The concentration independent rate constants ξ and ξ' can be calculated from the measured rate constants (k and k') and the equilibrium concentration of acetone and DMSO. Because there is a negligible amount of free chloroform in the mixed solvent, the equilibrium concentration of the complexes can be calculated using the initial concentration of chloroform and the measured population ratio, [chloroform−acetone]/[chloroform−DMSO] = 0.66. The calculated equilibrium concentrations of the four principal species are [chloroform−acetone] = 0.26 mol/L, [chloroform−DMSO] = 0.17 mol/L, [acetone] = 10.9 mol/L, and [DMSO] = 1.9 mol/L. The resulting equilibrium constant for the reaction (2) is 0.26. All of these values play important roles in interpreting the experimentally measured rates and calculating the rates of the elementary processes.

From the 2D-IR spectra, the volume of each peak was determined by fitting all of the peaks with two-dimensional Gaussian functions.[20,21] The fitting functions were not constrained to be symmetric, and therefore could account for the spectral diffusion of each peak. The derived volumes of the 4 peaks at 17 different T_wʼs were converted to normalized populations. From the IR experiments, the absorption coefficient for the chloroform−DMSO complex is 2.5 times larger than that of the chloroform−acetone complex, and the measured volumes were be properly normalized to compensate for transition dipole differences among the peaks. The transition dipole differences depend on the quantum pathways which describe each of the four peaks. The detailed explanation of how each peak is generated in the 2D-IR spectrum and the response function for each of the four peaks have already been published including the modifications to the elementary theory

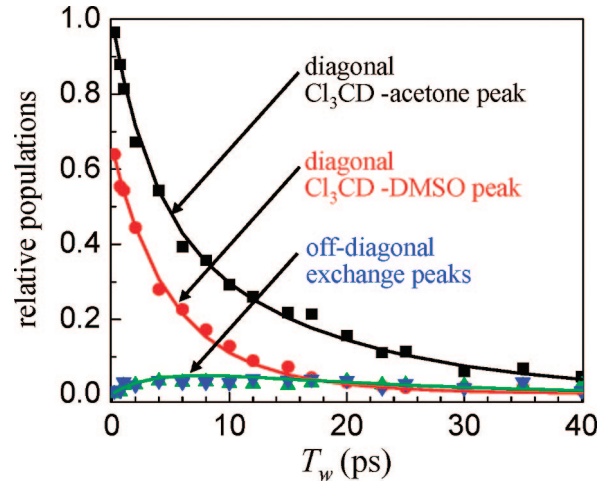

Figure 5. The symbols are the time dependent volumes of the four peaks seen in Figure 4. The solid lines through the data are the results of fitting the kinetic model to the data (see text). The results yield the chemical exchange times for partner switching between the $CDCl_3$−DMSO and $CDCl_3$−acetone complexes.

TABLE 1: Vibrational Lifetimes (T_1) and Orientational Relaxation Time Constants (τ_r) of the $CDCl_3$-Acetone and $CDCl_3$−DMSO Complexes[a]

solvent	T_1(ps)	τ_r(ps)
acetone	16	4 (4)
dimethylsulfoxide (DMSO)	8	16 (6)

[a] The τ_r values in parentheses are the times used in the data analysis, see text.

to account for chemical exchange.[20,21] The diagonal peak for the chloroform−DMSO complex is divided by the square of the absorption coefficient ratio, 2.5^2, because the absorption coefficient is proportional to the square of the transition dipole, and the diagonal 2D-IR peak is proportional to the fourth power of the transition dipole. The two off-diagonal peaks are proportional to the product squared of the chloroform−DMSO and chloroform−acetone transition dipoles. Thus the off-diagonal peaks are divided by the absorption coefficient ratio between the two complexes, 2.5. This normalization removes the influence of transition dipole differences from the data analysis.

Figure 5 shows the T_w dependence of the four peaks (symbols) in the 2D-IR spectra. The data are normalized to the largest peak at the shortest time, that is, the chloroform−acetone peak at $T_w = 0.2$ ps in a manner such that this peak begins at 1 at $T_w = 0$. The symbols in Figure 5 are the relative populations of peaks. To reduce the number of parameters used for fitting the observed population to the kinetic equations, the vibrational lifetimes and orientational relaxation times were measured separately using polarization selective IR pump−probe spectroscopy (see Table 1). The C−D stretch vibrational lifetimes were used as measured for the chloroform−acetone complex in pure acetone and the chloroform−DMSO complex in pure DMSO. The orientational relaxation time for the chloroform−acetone complex in pure acetone is expected to be virtually the same as the orientation time of the chloroform−acetone complex in the mixed solvent because the mixed solvent is primarily composed of acetone. However, the chloroform−DMSO complex experiences a different environment in the mixed solvent than it does in pure DMSO. This difference is illustrated by the large change in viscosity from 2 to 0.4 cP. The orientational relaxation time can be estimated from the measured orientational

relaxation time by using the Debye−Stokes−Einstein equation (DSE); however, this equation is not always appropriate for highly associative solvents. The DSE equation yields an orientational relaxation time in the mixed solvent of 3.2 ps. As an alternative, the orientational relaxation time for the chloroform−DMSO complex was treated as fitting variable in the global analysis with an upper limit set to the measured value from the pure DMSO. This resulted in 6 ps. Because both of these values are fast compared to the chemical exchange dynamics, the results are insensitive to the exact value.

The measured time-dependent peak volumes given in Figure 5 are fitted with the substitution rate constant, k, for

$$Cl_3CD\cdots O{=}S(CH_3)_2 \xrightarrow{k} Cl_3CD\cdots O{=}C(CH_3)_2$$

The other substitution rate constant is related to k by the equilibrium between [chloroform−DMSO] and [chloroform−acetone], so it is set as $k' = 0.66 \times k$. Therefore, it is only necessary to fit k. The best fit substitution rate constant is $k = 1/30\ ps^{-1}$. In other words, it takes 30 ps for $CDCl_3$ to change its hydrogen bonding partner from DMSO to acetone and 45 ps for $CDCl_3$ to changes its hydrogen bonding partner from acetone to DMSO ($k' = 1/45\ ps^{-1}$). Also, using these measured rate constants and the equilibrium concentrations of acetone and DMSO the second order rate constants (see Reaction 2) are, $\xi = 3.1 \times 10^{-3}\ (ps\cdot mol/l)^{-1}$and $\xi' = 1.2 \times 10^{-2}\ (ps\cdot mol/l)^{-1}$. As discussed above, the chloroform−DMSO orientational relaxation time was also fit and yielded 6 ps. The values of the rate constants are unchanged when the orientational relaxation time was fixed at the DSE value of 3.2 ps, and a single adjustable parameter, k, is used in the fits.

The information obtained from the 2D-IR CES experiments are the exchange times (inverses of the rate constants) for the two complexes under equilibrium conditions. As discussed above, the presence of free $CDCl_3$ suggests that the chemical exchange proceeds through the free species as an intermediate. This model will be confirmed by the analysis presented below. In this model, the exchange in one direction occurs by dissociation of a chloroform−acetone complex to form free chloroform, diffusion to bring free chloroform into proximity with DMSO, and formation of the chloroform−DMSO complex. The exchange in the other direction occurs by dissociation of a chloroform−DMSO complex to form free chloroform, diffusion to bring free chloroform into proximity with acetone, and formation of the chloroform−acetone complex. The entire substitution reaction can be written as three basic processes.

$$\begin{aligned} Cl_3CD\cdots O{=}S(CH_3)_2 &\underset{k_f^D}{\overset{k_d^D}{\rightleftharpoons}} CDCl_3^{(D)} + O{=}S(CH_3)_2 \\ CDCl_3^{(D)} &\underset{k'_{diff}}{\overset{k_{diff}}{\rightleftharpoons}} CDCl_3^{(A)} \\ CDCl_3^{(A)} + O{=}C(CH_3)_2 &\underset{k_d^A}{\overset{k_f^A}{\rightleftharpoons}} Cl_3CD\cdots O{=}C(CH_3)_2 \end{aligned} \quad (4)$$

k_d^D and k_f^D are the dissociation and formation rate constants, respectively for the complex with DMSO. k_d^A and k_f^A are the dissociation and formation rate constants, respectively for the complex with acetone. k_{diff} and k'_{diff} are the diffusion controlled rate constants for chloroform and acetone to encounter each other and chloroform and DMSO to encounter each other, respectively. The superscripts (A) and (D) above $CDCl_3$ denote that the $CDCl_3$ has not yet diffused away from an acetone or DMSO to which it was previously hydrogen bonded. It is expected that the dissociation of the hydrogen-bonded chloroform−DMSO complex is much slower than that of the hydrogen-bonded chloroform−acetone complex because chloroform forms a substantially stronger hydrogen bond with DMSO than it does with acetone. Previous work on other hydrogen-bonded complexes has shown that the dissociation time increases exponentially as the enthalpy of formation of the complex increases.[20,24,39] The diffusion controlled rates for free chloroform to find an acetone or DMSO can be calculated using a Smoluchowski treatment for diffusion controlled reactions.[43−45] Therefore, reasonably accurate estimates can be obtained for the steps in kinetic eq 4.

Kinetic eq 4 illustrates a process where the substitution reaction for the hydrogen bonding partner of chloroform proceeds through an intermediate, free chloroform, in a manner similar to an S_N1 reaction scheme. Depending on the details of the system, either breaking a bond to form the intermediate or the diffusive encounter of the intermediate with a new partner can be the rate limiting step. Because the chloroform−DMSO hydrogen bond is strong and acetone is in very high concentration, we expect breaking of the bond to dominate the time dependence of the chloroform−DMSO → chloroform−acetone half-reaction. In contrast, because the chloroform−acetone hydrogen bond is weak and DMSO is relatively low in concentration, we expect the diffusive encounter to dominate the time dependence of the chloroform−acetone → chloroform−DMSO half-reaction. Even though the rates for the elementary steps in kinetic eq 4 cannot be measured independently, we can obtain very good estimates and confirm those estimates.

The dissociation time of a complex (hydrogen bond breaking) should be independent of the reactant concentrations. Consider the result of increasing the concentration of acetone until the solution is virtually pure acetone with only small number of chloroform−DMSO complexes. Because the chloroform−DMSO is completely surrounded by acetone, free chloroform formed after breaking the hydrogen bond with DMSO requires almost no time to find an acetone with which to hydrogen bond. The rate of the entire reaction in this case is close to the rate of breaking the hydrogen bond between the chloroform and DMSO. This idealized rate for an essentially pure acetone sample is calculated using the approximation $k_d^D \cong \xi \times [\text{acetone}]$. Using the 2D-IR CES measured ξ and the concentration of pure acetone, 13.6 mol/L results in 24 ps for the chloroform−DMSO dissociation time ($1/k_d^D$, see kinetic eq 4). Also using the measured ξ' and the concentration of pure DMSO, 14.08 mol/L, the chloroform−acetone dissociation time is 6 ps ($1/k_d^A$, kinetic eq 4). These two rate constants, $k_d^D = 1/24$ ps and $k_d^A = 1/6$ ps, corresponds to the two elementary reaction rate constants for steps in the top and bottom equations of kinetic eq 4. The difference between the dissociation time and the 2D-IR chemical exchange time is the time for the diffusive encounter. Therefore, when chloroform−DMSO dissociates it takes 6 ps for the free chloroform to encounter and bond to an acetone (30−24 ps), and when chloroform−acetone dissociates it take 39 ps for the free chloroform to encounter and bond to an DMSO (45−6 ps).

The mechanism embodied in kinetic eq 4 and the values for the elementary steps estimated above can be checked by performing a simple diffusion controlled rate calculation using the Smoluchowski equation.[45] Combining the Smoluchowski equation and the Stokes−Einstein equation for the diffusion coefficient and using the fact that the species have similar radii,

gives the diffusion controlled reaction rate coefficient, $k_D = 8RT/3\eta$.[45] The viscosity of the mixed solvent η is 0.4 cP, and k_D is determined to be 1.66×10^{-2} $(ps)^{-1}(mol/L)^{-1}$. This is the second-order rate coefficient for free chloroform to encounter another reactant, DMSO or acetone. Thus the equilibrium concentration should be multiplied by this constant to determine the rate constants in the middle equation of kinetic eq 4. The diffusion controlled rate for the free chloroform to encounter DMSO is $k_{diff} = k_D \times [DMSO]$, 1/32 $(ps)^{-1}$. Thus it takes ~32 ps for free chloroform from an acetone complex to encounter a DMSO molecule. This time should be compared with 39 ps determined above, which corresponds to the difference between the measured chloroform−DMSO to chloroform−acetone chemical exchange time (45 ps, inverse of the rate constant) and the hydrogen-bonding dissociation time (inverse of the rate constant) estimated above to be 6 ps. The two times obtained for the diffusion controlled rate constant from agree well with each other. Also, the diffusion controlled rate constant for free chloroform from a DMSO complex to find an acetone molecule is $k'_{diff} = k_D \times [acetone]$, 1/5.5$(ps)^{-1}$, which means it takes ~5.5 ps for free chloroform from a DMSO complex to encounter an acetone molecule. This also matches well with the difference between the measured chloroform−acetone to chloroform−DMSO chemical exchange time (30 ps) and the hydrogen bonding dissociation time estimated above to be 24 ps.

The agreement between the Smoluchowski equation calculations and the experimentally determined values confirms that the hydrogen bond acceptor substitution reaction proceeds through a S_N1 type reaction mechanism with free chloroform as the reactive intermediate. Thus, we are able to reasonably separate the hydrogen bond dissociation times of the complexes and the diffusive encounter times. The results give the chloroform−DMSO hydrogen bond dissociation time, $1/k_d^D$ = 24 ps, and the chloroform−acetone hydrogen bond dissociation time, $1/k_d^D$ = 6 ps.

III. Concluding Remarks

The hydrogen bonding partner substitution reaction has been studied using ultrafast 2D-IR vibrational echo chemical exchange spectroscopy. Through the analysis of IR absorption spectra, it was shown that DMSO primarily exists as a cyclic dimer even in the mixed DMSO/acetone solvent which is mainly composed of acetone. When $CDCl_3$ is dissolved in the mixed solvent, it forms hydrogen-bonded complexes (C−D···O=) with DMSO cyclic dimers and acetone cyclic dimers. The strength of the hydrogen bond is weak so $CDCl_3$ can switch its hydrogen bonding partner from DMSO to acetone and vice verse even at room temperature. The substitution reaction rates are measured from the growth of the off-diagonal peaks in a series of time dependent 2D-IR spectra. For the composition of the sample studied in this paper, chloroform−DMSO interconverts to chloroform−acetone in 30 ps, and chloroform−acetone converts to chloroform−DMSO in 45 ps. The free chloroform (not complexed) acts as a reactive intermediate in the S_N1 type substitution reaction which involves three elementary steps. From the measured rates which depend on the reactant concentrations, the rates of the elementary steps of hydrogen bond breaking of the two types of dimers were determined with reasonable accuracy. It was found that the dissociation time for the chloroform−DMSO complex is 24 ps and for the chloroform−acetone complex it is 6 ps. The differences between the total reaction rates and the dissociation rates were shown to be consistent with a diffusive reaction process described in terms of a simple Smoluchowski treatment of the S_N1 chloroform−DMSO ↔ chloroform−acetone substitution reaction.

The results presented here provide the first measurement of the time scale for the dissociation of C−D hydrogen bonded to oxygen. Hydrogen bonds involving a C−H are important in chemistry and biology.[2,3] For the weak hydrogen bond between $CDCl_3$ and acetone, the time is ~6 ps and for the stronger hydrogen bond formed with DMSO the time is ~24 ps. The times scales for C−H instead of C−D should be the same. These times can be compared to the dissociation times of an alcohol hydroxyl group π-hydrogen bonded to an aromatic.[20,24,39] The times measured here fall in the fast to moderate range of the times measured in the alcohol systems. For example the dissociation time of the phenol/bromobenzene complex is 5 ps and the phenol/p-xylene complex is 24 ps.[20,24,39] For alcohols, the dissociation times are very correlated to the enthalpies of formation of the complexes, ΔH^0.[24,39] For the phenol/bromobenzene complex $\Delta H^0 = -1.2$ kcal/mol, and for the phenol/p-xylene complex $\Delta H^0 = -2.2$ kcal/mol. If the same correlation holds for the C−D hydrogen bonds, then these ΔH^0 are estimates of the enthalpies of formation of the chloroform−acetone and chloroform−DMSO hydrogen-bonded complexes.

We have shown the C−H hydrogen bonds can be studied using the 2D-IR vibrational echo chemical exchange spectroscopy using the C−H or C−D stretching mode. The 2D-IR signal from the hydrogen-bonded C−D band dominates the signal from non-hydrogen-bonded C−Ds because of the large enhancement of transition dipole upon the formation of the hydrogen bond. Thus the hydrogen bond itself works as a label in a 2D-IR experiment without the need to incorporate a non-native label. Going a step further, selective deuteration would enable 2D-IR vibrational echo experiments to observe the C−H hydrogen bond dynamics of a chosen substructure of a macromolecule.

Acknowledgment. We would like to thank the Air Force Office of Scientific Research (F49620-01-1-0018), the National Science Foundation (DMR 0652232), and the National Institutes of Health (2-R01-GM061137-09) for support of this work. D.E.R. is supported by the Fannie and John Hertz Foundation and a Stanford Graduate Fellowship.

References and Notes

(1) Green, R. D. *Hydrogen Bonding by C-H Groups*; John Wiley & Sons: New York, 1974.
(2) Desiraju, G. M. *The Weak Hydrogen Bond in Structural Chemistry and Biology*; Oxford University Press: New York, 1999.
(3) Nisiho, M. *The Ch-P Interaction: Evidence, Nature, and Consequences*; Wiley: New York, 1998.
(4) Allen, F. H.; Kennard, O.; Taylor, R. *Acc. Chem. Res.* **1983**, *16*, 146.
(5) Desiraju, G. R. *Acc. Chem. Res.* **1996**, *29*, 441.
(6) Steiner, T. *Acta Crystallogr.* **1995**, *D51*, 93.
(7) Lutz, B.; Kanters, J. A.; Mass, J. v. d.; Kroon, J.; Steiner, T. *J. Mol. Struct.* **1998**, *440*, 81.
(8) Ding, S.; Hong, Y.-W.; Chen, C.-Y.; Chang, N.-C. *Biophys. Chem.* **2006**, *121*, 75.
(9) Huggins, C. M.; Pimentel, G. C. *J. Chem. Phys.* **1955**, *23*, 1244.
(10) Tkadlecova, M.; Dohnal, V.; Costas, M. *Phys. Chem. Chem. Phys.* **1999**, *1*, 1479.
(11) Schneider, W. G.; Bernstein, H. J.; Pople, J. A. *J. Chem. Phys.* **1958**, *28*, 601.
(12) Pimentel, G. C.; McClellan, AL. *Annu. Rev. Phys. Chem.* **1971**, *22*, 347.
(13) Daniel, D.; Mchale, J. L. *J. Phys. Chem. A* **1997**, *101*, 3070.
(14) Huggins, C. M.; Pimentel, G. C. *J. Am. Chem. Soc.* **1955**, *23*, 896.
(15) Senes, A.; Ubarretxena-Belandia, I.; Engelman, D. M. *Proc. Natl. Acad. Sci. U.S.A.* **2001**, *98*, 9056.
(16) Arbely, E.; Arkin, I. T. *J. Am. Chem. Soc.* **2004**, *126*, 5362.
(17) Corey, E. J.; Lee, T. W. *Chem. Comm.* **2001**, 1321.
(18) Lersch, M.; Tilset, M. *Chem. Rev.* **2005**, *105*, 2471.
(19) Kim, Y. S.; Hochstrasser, R. M. *Proc. Natl. Acad. Sci. U.S.A.* **2005**, *102*, 11185.

(20) Zheng, J.; Kwak, K.; Asbury, J. B.; Chen, X.; Piletic, I.; Fayer, M. D. *Science* **2005**, *309*, 1338.
(21) Kwak, K.; Zheng, J.; Cang, H.; Fayer, M. D. *J. Phys. Chem. B* **2006**, *110*, 19998.
(22) Zheng, J.; Kwak, K.; Chen, X.; Asbury, J. B.; Fayer, M. D. *J. Am. Chem. Soc.* **2006**, *128*, 2977.
(23) Zheng, J.; Kwak, K.; Xie, J.; Fayer, M. D. *Science* **2006**, *313*, 1951.
(24) Zheng, J.; Fayer, M. D. *J. Am. Chem. Soc.* **2007**, *129*, 4328.
(25) Zheng, J.; Kwak, K.; Fayer, M. D. *Acc. Chem. Res.* **2007**, *40*, 75.
(26) Ishikawa, H.; Kwak, K.; Chung, J. K.; Kim, S. *Proc. Natl. Acad. Sci. U.S.A.* **2008**, *105*, 8619–8624.
(27) DeCamp, M. F.; DeFlores, L.; McCracken, J. M.; Tokmakoff, A.; Kwac, K.; Cho, M. *J. Phys. Chem. B* **2005**, *109*, 11016.
(28) Kobayashi, K.; Kanesaka, I. *J. Raman Spectrosc.* **2007**, *38*, 436.
(29) Srivastava, S. K.; Ojha, A. K.; Koster, J.; Shukla, M. K.; Lsezczynski, J.; Asthana, B. P.; Kiefer, W. *J. Mol. Struct.* **2003**, *661*, 11.
(30) Czeslik, C.; Jonas, J. *J. Phys. Chem. A* **1999**, *103*, 3222.
(31) Amey, R. L. *J. Phys. Chem.* **1968**, *72*, 3358.
(32) Sastry, M. I. S.; Singh, S. *J. Raman Spectrosc.* **1984**, *15*, 80.
(33) Matin, D.; Weise, A.; Niclas, H. J. *Angew. Chem., Int. Ed.* **1967**, *6*, 318.
(34) Rintoul, L.; Shurvell, H. F. *J. Raman Spectrosc.* **1990**, *21*, 501.
(35) Becker, E. D. *Spectrochim. Acta* **1959**, 743.
(36) Kagarise, R. E. *Spectrochim. Acta* **1963**, *19*, 629.
(37) Geller, B. A.; Skrunts, L. K. *Theor. Exp. Chem.* **1973**, 556.
(38) Person, W. B. *J. Chem. Phys.* **1958**, *28*, 319.
(39) Zheng, J.; Fayer, M. D. *J. Phys. Chem. B* **2008**, *112*, 10221.
(40) Kwac, K.; Lee, C.; Jung, Y.; Han, J.; Kwak, K.; Zheng, J.; Fayer, M. D.; Cho, M. *J. Chem. Phys.* **2006**, *125*, 244508.
(41) Park, S.; Kwak, K.; Fayer, M. D. *Laser Phys. Lett.* **2007**, *4*, 704.
(42) Marcus, Y. *Solvent Mixture*; Marcel Dekker: New York, 2002.
(43) Berry, R. S.; Rice, S. A.; Ross, J. *Physical Chemistry*; Oxford University Press: Oxford, 2000.
(44) Atkins, P. W. *Physical Chemistry*, 5th ed.; W.H. Freeman: New York, 1994.
(45) Levine, I. N. *Physical Chemistry*, 5th ed.; McGraw-Hill: New York, 2002.

JP806035W